

Lifting of a large object from a porous seabed

By CHIANG C. MEI,

Department of Civil Engineering, Massachusetts Institute of Technology

RONALD W. YEUNG

Department of Naval Architecture and Offshore Engineering,
University of California at Berkeley

AND KO-FEI LIU

Department of Civil Engineering, Massachusetts Institute of Technology

(Received 6 October 1982 and in revised form 11 May 1984)

The time required to pull a large object from a sandy seabed is estimated by assuming that the seabed is porous but rigid. The phenomenon of *breakout* (i.e., sudden release) is shown to occur without the assumption of elasticity of the soil skeleton (Foda 1982). A new case of wedge-shaped gap is also studied, and compared to a uniform gap. Laboratory experiments are shown to support the theory.

1. Introduction

In the positioning of a large caisson or a gravity platform, the operating of submarines, or the salvaging of sunken ships, it is useful to know the time required to lift the object off the sea bottom for a prescribed vertical force. From field experience, it is known that the initial increase of the gap between the object and the seabed is a very slow process, until a critical time when the object is broken loose suddenly. This phenomenon is called *breakout*. Because of its importance in the operation and rescue of submarines, a research project was carried out by the U.S. Naval Civil Engineering Laboratory at Port Hueneme, California during 1965–68. Field tests were conducted in San Francisco Bay and the Gulf of Mexico for objects that were allowed to settle into the soil for some time. At these places the seabed is composed of silty clay whose permeability is extremely low. From these data Liu (1969) proposed an empirical formula relating the breakout force and time for mud; the scatter of measured data was, understandably, rather large. Liu also suggested three possible mechanisms for breakout: (1) Soil shear failure. When the interior shear stress exceeds the yield strength, fractures develop, leading to failure. (2) Soil tension failure. If the top layer of the soil is fine clay, fluid saturation diminishes the cohesive strength of mud. (3) Failure of adhesion between soil and the object. This is the dominant mechanism when the top soil is sandy and the object surface is smooth.

It is evident that different theories are needed for different soil environments. Muga (1968) reported a two-dimensional numerical theory which was aimed at the shear failure mechanism; he treated the soil as a one-phase elastic/perfect-plastic continuum. The soil/object bond was assumed to be infinite. To study the third mechanism, i.e. loss of bonding between soil and object, Harleman & Shamir (1963, private communication) have performed two-dimensional tests on a saturated sandbed in a pail. They examined circular cylinders pressed into the sandbed to a depth of $\frac{1}{2}$ or

$\frac{1}{3}$ -cylinder radius. Their data were also quite scattered. Relevant theories were not available until recently.

If the seabed is regarded as a rigid and impervious half space with a plane top, then the time required to pull up a circular disk of radius a from height h_0 to height h is known to be

$$t = \frac{3\pi\mu a^4}{4F} \left(\frac{1}{h_0^2} - \frac{1}{h^2} \right), \quad (1.1)$$

according to the lubrication theory (Batchelor 1967, p. 228), where F is the applied vertical force and μ the viscosity of water. This formula shows, however, no sudden change of dh/dt at any time. If the initial height h_0 is zero, the time for pulling away the disk would be infinite. Clearly other physical factors must be considered. Now, for a sandy soil fluid can be withdrawn from within the seabed when the object is lifted up. This tends to reduce the suction in the gap and the time for breakout. Foda (1982) has proposed a theory which takes into account not only porosity but also the elasticity of the seabed. In his theory, a boundary-layer approximation of Mei & Foda (1981) was employed which asserted that the fluid flow in a porous seabed of small permeability was largely confined within a thin layer near the mud line, if the final time of breakout was much shorter than the consolidation time of the seabed. The remainder of the seabed was deformed but did not yield fluid to the gap. Despite this approximation, the ensuing analysis was rather complex. In order to avoid lengthy computation of the elastic response of the soil skeleton, the displacement of the mud line directly beneath the gap was further assumed to be uniform, which likely introduced some quantitative inaccuracy. Also it is unclear whether the two physical factors considered by Foda, porosity and soil deformation, are of equal importance in the breakout from a sandy seabed under practical conditions, there being no comparison with well-controlled experiments.

For sufficiently small uplift force per unit contact area or for relatively strong soils, one expects that the seabed can be treated as being porous but rigid. In this paper first we shall consider theoretically such a simple model for the loss of adhesion between an impervious body and the seabed, with a view to (1) providing mathematically accurate solutions, (2) examining whether soil elasticity is qualitatively essential to breakout, and (3) studying the new case of a wedge-shaped gap. Instead of the continuity of the horizontal velocities at the soil-water interface as assumed by Foda, we shall apply the boundary condition found experimentally by Beavers & Joseph (1967), and justified theoretically by Saffman (1971), which implies a thin boundary layer in the porous solid. Although unpublished experimental data exist for a circular cylinder (Harleman & Shamir), the difference in geometry and the considerable experimental scatter prevent a meaningful comparison with theory. We shall therefore describe our own experiments on a saturated sand layer for an object with a flat bottom. Comparison with, and the practical relevance of, the rigid bed theory are discussed.

2. Two-dimensional analysis

We assume the bottom of the body and the top of the seabed, i.e. the *mud line*, to be flat. If $p(x, t)$ is the hydrodynamic pressure in the gap, then, by assuming creeping flow, the corresponding velocity within the gap is

$$u(x, y, t) = \frac{y^2}{2\mu} \frac{\partial p}{\partial x} + Ay + B. \quad (2.1)$$

In the porous seabed, the fluid is assumed to be incompressible

$$\nabla \cdot \mathbf{u}_- = 0, \quad (2.2)$$

and the flow obeys Darcy's law

$$\mathbf{u}_- = -\frac{k}{\mu} \nabla \phi = \frac{k}{\mu} \left(-\frac{\partial \psi}{\partial y}, \frac{\partial \psi}{\partial x} \right), \quad (2.3)$$

where \mathbf{u}_- is the seepage velocity in the seabed, ϕ the pore pressure, ψ the stream function, μ the fluid viscosity and k the permeability. The pore pressure and stream function are harmonic if k and μ are constants, which we assume.

At the moving bottom of the body $y = h(x, t)$, no slipping is allowed; hence:

$$u = 0 \quad \text{for uniform gap} \quad (2.4a)$$

$$= -\frac{dH}{dt} \frac{xH}{L^2} \quad \text{for wedged gap} \quad (2.4b)$$

$$\left. \vphantom{\begin{matrix} (2.4a) \\ (2.4b) \end{matrix}} \right\} 0 < x < L$$

where H is the maximum gap height at any t and L is the length of the gap. In the second (wedged gap) case, the edge at $x = 0$ is supposed to be always in contact with the soil (see figure 1). Since the slope H/L is anticipated to be small, $u = 0$ can be applied to both gaps with sufficient accuracy, as is explained later.

As for the kinematic condition on the horizontal velocity at the bottom of the gap ($y = 0$), Beavers & Joseph argue that there is a thin boundary layer below $y = 0$. If u_- denotes the horizontal velocity just below the boundary layer, then

$$\frac{\partial u}{\partial y} = \alpha k^{-\frac{1}{2}}(u - u_-), \quad 0 < x < L, \quad y = 0 \quad (2.5)$$

where α is an empirical constant depending on the structure of the porous material, but is largely independent of viscosity. By regarding the boundary as the limit of a sharply changing inhomogeneous porous layer, theoretical justification of (2.5) has been given by Saffman (1971), who also points out that to lead order it is sufficient to use

$$\frac{\partial u}{\partial y} = \alpha k^{-\frac{1}{2}} u, \quad 0 < x < L, \quad y = 0 \quad (2.6)$$

since u_- is of the order $O(k)$ relative to u . Experiments by Beavers & Joseph for nickel foamets† with $k = (1.0, 4.0, 8.2) \times 10^{-4} \text{ cm}^2$ gave $\alpha = 0.78, 1.45, 4.0$, respectively. For aloxities† with $k = 6.5 \times 10^{-6}$ and $1.6 \times 10^{-5} \text{ cm}^2$, $\alpha = 0$. The range of permeabilities for sandy soils is very wide: from $k = 10^{-8} \text{ cm}^2$ for fine sand to 10^{-5} cm^2 for coarse sand. By extrapolation from a log-log plot, we estimate the corresponding value for α to be about 0.001 for very fine sand and 0.1 for coarse sand. More reliable values must await future experiments.

Use of (2.4b) and (2.6) in (2.1) yields

$$u = \frac{1}{2\mu} \frac{\partial p}{\partial x} y^2 + \left(-\frac{dH}{dt} \frac{xH}{L^2} - \frac{h^2}{2\mu} \frac{\partial p}{\partial x} \right) \frac{1 + \alpha y k^{-\frac{1}{2}}}{1 + \alpha h k^{-\frac{1}{2}}} \quad (2.7)$$

for a wedged gap. For a uniform gap we simply omit the term $-(dH/dt)(xH/L^2)$ and replace all h by H in (2.7).

† Foametal has a cellular structure consisting of irregularly shaped interconnected pores formed by a lattice construction, whereas aloxite is made from fused crystalline aluminum oxide grains held together with a ceramic bond (Beavers & Joseph, 1976).

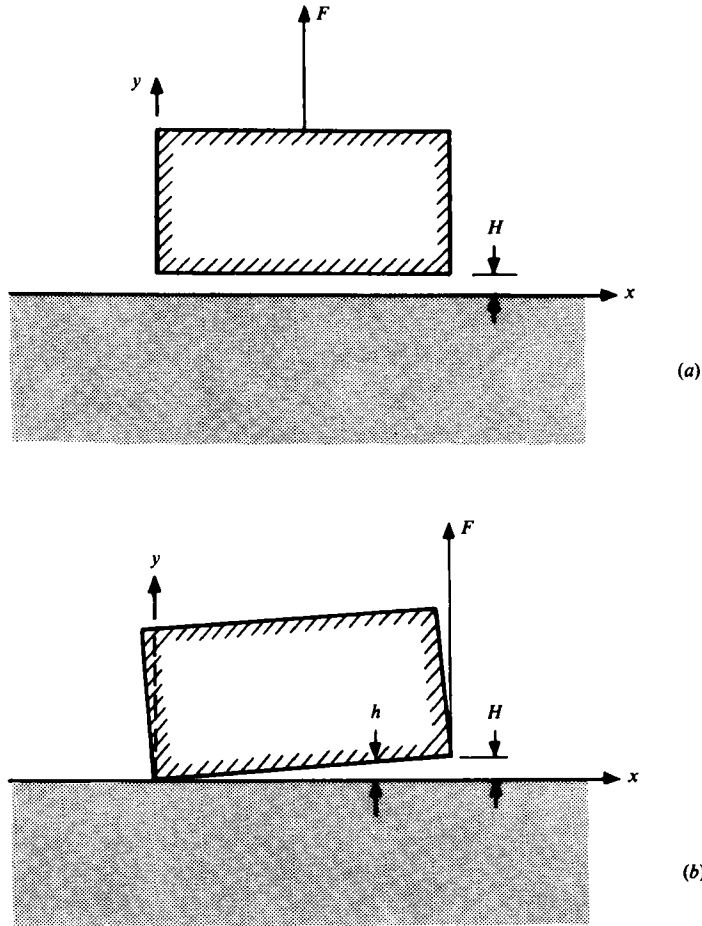


FIGURE 1. Definition sketches: (a) uniform gap, (b) wedged gap.

By integrating the continuity equation for the gap fluid from $y = 0$ to $y = h$ we get

$$\frac{dh}{dt} = v_-(x, 0, t) - \frac{\partial}{\partial x} \int_0^h u \, dy + \frac{\partial h}{\partial x} u(x, h, t), \tag{2.8}$$

after using the Leibniz rule. Substituting (2.7) in (2.8) we see readily that the $-(dh/dt)(xH/L^2)$ term in (2.7) gives a contribution of $O(H/L)^2$ compared to the left-hand side dh/dt . Hence we shall omit this term from (2.7) and (2.8); this omission amounts to letting $u = 0$ at $y = h$ for a wedged gap also, as anticipated in the sentence following (2.4*b*). With this omission, we integrate (2.8) with respect to x to get

$$\int_{x_0}^x dx \frac{dh}{dt} = \frac{k}{\mu} \psi(x, 0, t) - \int_0^h u \, dy, \tag{2.9}$$

where the point x_0 is chosen so that

$$\int_0^h u \, dy = 0 \quad \text{at } x = x_0.$$

At the same point x_0 we also define

$$\psi(x_0, 0, t) = 0.$$

For a uniform gap, we must take x_0 to be at the centre line

$$x_0 = \frac{1}{2}L; \tag{2.10}$$

while for a wedged gap, we choose the left end, which is assumed to be contact with the soil surface at all times:

$$x_0 = 0. \tag{2.11}$$

Outside the gap, the dynamic pressure in the fluid above the seabed can be approximated by zero, as is the usual practice in the theory of lubrication. Thus,

$$p = \phi = 0, x < 0 \quad \text{and} \quad x > L, y = 0. \tag{2.12}$$

Since ϕ and ψ are harmonic conjugates, Cauchy's formula gives

$$\psi(x, 0, t) = \frac{1}{\pi} \int_0^L \frac{\phi(x', 0, t)}{x' - x} dx', \tag{2.13}$$

where the right-hand side is a principal-valued integral (Morse & Feshbach 1952 vol. I, p. 371). Invoking the continuity of pressure along $0 < x < L, y = 0$, we get

$$\left\{ \begin{array}{l} (x - \frac{1}{2}L) \\ x^2 \\ 2L \end{array} \right\} \frac{dH}{dt} = \frac{k}{\mu} \frac{1}{\pi} \int_0^L \frac{p(x') dx'}{x' - x} - \frac{\partial p}{\partial x} \frac{h^3}{2\mu} \left(\frac{1}{3} - \frac{1 + \alpha h / 2k^2}{1 + \alpha h / k^2} \right), \tag{2.14}$$

with
$$h = \left\{ \begin{array}{l} H(t) \\ H(t) \frac{x}{L} \end{array} \right\} \tag{2.15}$$

for (uniform/wedged) gap, respectively.

Let F be the applied vertical force per unit length in the z direction in excess of the buoyant weight of the body; then total force balance requires that

$$\int_0^L p(x) dx = -F \tag{2.16}$$

for the uniform gap. For the wedged gap we assume that F is applied along the edge $x = L$; moment balance requires that

$$\int_0^L xp(x) dx = -FL. \tag{2.17}$$

The restoring moment due to the buoyant weight is excluded. Equation (2.14) is an integro-differential equation for $p(x, t)$ and $H(t)$. It must be supplemented with the boundary condition

$$p(L, t) = 0 \quad t > 0 \tag{2.18}$$

and the initial condition

$$H(0) = 0. \tag{2.19}$$

Equation (2.14) states, of course, that the rate of increase in water mass between $x = x_0$ and $x = x$ equals the sum of the upward flux from the soil and the inward flux

from the edges. Now the characteristic physical quantities of this problem are F, L, k and μ . Let T be the timescale for breakout; then from (2.14) the order relationship

$$\frac{LH}{T} \sim \frac{kF}{\mu L} \sim \frac{F H^3}{L^2 \mu} \tag{2.20}$$

must follow. Eliminating H , we get the dependence of T on the physical parameters

$$T = C \left(\frac{\mu L^{\frac{3}{2}}}{F k^{\frac{3}{2}}} \right). \tag{2.21}$$

The coefficient C should be of order unity; its precise value requires the explicit solution of (2.14).

3. Method of numerical solution

If the following non-dimensional variables are introduced:

$$P = pL/F, \quad \xi = x/L, \quad \sigma = (Lk)^{-\frac{1}{2}}h, \quad \tau = (Fk^{\frac{3}{2}}/\mu L^{\frac{3}{2}})t, \tag{3.1}$$

and if one defines
$$\frac{1}{\pi} B(\sigma, \beta) = \frac{\sigma^3}{2} \left(\frac{1}{3} - \frac{1 + \frac{1}{2}\beta\sigma}{1 + \beta\sigma} \right), \tag{3.2}$$

and
$$\beta = \alpha L^{\frac{1}{2}}/k^{\frac{1}{2}}, \tag{3.3}$$

(2.14) becomes
$$\frac{d\sigma}{d\tau} (\xi - \frac{1}{2}) = \frac{1}{\pi} \int_0^1 \frac{P(\eta) d\eta}{\eta - \xi} - \frac{1}{\pi} B(\sigma, \beta) \frac{\partial P}{\partial \xi}, \tag{3.4a}$$

with
$$\int_0^1 P(\xi) d\xi = -1 \tag{3.4b}$$

for a uniform gap. For a wedge gap, (2.14) becomes

$$\frac{d\sigma}{d\tau} \frac{\xi^2}{2} = \frac{1}{\pi} \int_0^1 \frac{P(\eta) d\eta}{\eta - \xi} - \frac{1}{\pi} B(\sigma\xi, \beta) \frac{\partial P}{\partial \xi}, \tag{3.5a}$$

with
$$\int_0^1 \xi P(\xi) d\xi = -1. \tag{3.5b}$$

Equations (3.4a) and (3.5a) depend only on a single (porosity) parameter β .

We should point out that B is always negative. For both gaps, the auxiliary (end) conditions (2.18) and (2.19) for P and initial condition for σ become, respectively,

$$P(1, \tau) = 0 \quad \tau > 0 \quad \sigma(0) = 0. \tag{3.6}, (3.7)$$

Since (3.4a) and (3.5a) have unknown left-hand sides and are linear in P , it is convenient to introduce an intermediate function

$$\tilde{P}_i(\xi, \tau) = \frac{P(\xi, \tau)}{\pi \sigma_i} \quad \begin{matrix} i = 0 \text{ uniform} \\ i = 1 \text{ wedged.} \end{matrix} \tag{3.8}$$

Hence
$$f_i(\xi) = \int_0^1 \frac{\tilde{P}_i(\eta) d\eta}{\eta - \xi} - B(\sigma\xi^i, \beta) \frac{\partial \tilde{P}_i}{\partial \xi} \tag{3.9}$$

with $f_0(\xi) = \xi - \frac{1}{2}$ and $f_1(\xi) = \frac{1}{2}\xi^2$. The total load or moment condition, (3.4b), (3.5b), then yield immediately:

$$\frac{d\sigma_i}{d\tau} = \frac{-1}{\pi \Gamma_i}, \quad \Gamma_i = \int_0^1 \xi^i \tilde{P}(\xi) d\xi \tag{3.10}, (3.11)$$

This procedure effectively decouples the dependence of the solution in space from time.

Typical calculations proceed as follows. At a given time, the latest value of σ is used to calculate $B(\sigma, \beta)$ in (3.9), which is solved by discretization in the interval $\xi = [0, 1]$. A linear approximation of the function $\tilde{P}_i(\xi)$ between successive grid points is used. The Cauchy integral is evaluated analytically; the first derivative is approximated by first-order differencing, and a linear system for (3.9) is solved. The end condition (3.6) is essential in the solution procedure. Once $d\sigma_i/d\tau$ is available from (3.10), the value of σ_i can be advanced and the procedure is repeated. In practice, it was found to be more convenient to prescribe the values of σ and advance τ instead.

Two special cases of (3.8) can be solved analytically. At $\tau = 0, \sigma = 0$; hence $B = 0$ and (3.8) reduces to the usual Cauchy integral equation well known in the theory of airfoils (Tricomi 1957, chap. 4). The uniform gap and wedged gap correspond to the cases of parabolic-arc and cubic-camber, respectively. The solutions are:

$$\tilde{P}_0(\xi) = \frac{-1}{\pi} [(1-\xi)\xi]^{\frac{1}{2}}, \quad \frac{d\sigma_0}{d\tau} = \frac{8}{\pi}; \tag{3.12a}$$

$$\tilde{P}_1(\xi) = \frac{-1}{16\pi} \left(\frac{1-\xi}{\xi} \right) [8\xi^2 + 4\xi + 3], \quad \frac{d\sigma_1}{d\tau} = \frac{16}{\pi}. \tag{3.12b}$$

These have been used to check the numerical results. In the limit of large value of σ where the Cauchy integral becomes negligible, the differential equation for $\tilde{P}_0(\xi)$ is elementary, and the solution is simply

$$\tilde{P}_0(\xi) = \frac{-1}{2B(\sigma_0, \beta)} [\xi^2 - \xi], \quad \frac{d\sigma_0}{d\tau} = \frac{-12B(\sigma_0, \beta)}{\pi}. \tag{3.13}$$

All numerical results of the uniform gap case were observed to approach this limit asymptotically and monotonically.

Finally, it is worth noting that by putting $\xi = 1$ in (3.4a) and (3.5a) we get

$$\frac{1}{2} \frac{d\sigma}{d\tau} = \frac{1}{\pi} \int_0^1 \frac{P(\eta) d\eta}{\eta-1} - \frac{B(\sigma, \beta)}{\pi} \left. \frac{\partial P}{\partial \xi} \right|_{\xi=1}, \tag{3.14}$$

which is the equation of mass conservation in the region ($\frac{1}{2} < \xi < 1$) for a (uniform/wedged) gap. Note that the second term on the right of (3.14), which corresponds to the horizontal flux from the edge at $x = L$, is always positive for all $\sigma > 0$.

4. Numerical results

For sands, $k = 10^{-8} - 10^{-5} \text{ cm}^2$; the estimated range for α is 0.001– 0.125. The corresponding range of β is 0.1 to 3.16 for $L = 10^2 \text{ cm}$ and 0.1 to 6.8 for $L = 10^3 \text{ cm}$. Sample variations of the dimensionless gap width with time are given in figure 2 for a uniform gap for $\beta = 0.1, 1, 10, \text{ and } 100$. The last case, $\beta = 100$, is practically the limit of $\beta \rightarrow \infty$ where the no-slip boundary condition $u = 0$ applies on $0 < x < L, y = 0$ instead of (2.6). A breakout time can be defined by the vertical asymptote for each case from the plot. Clearly, pulling at one edge of the body is vastly more effective than pulling at the centre. Note that the initial portion of the $\log_{10} \sigma$ vs. $\log_{10} \tau$ curve is straight with unit slope, and is independent of β . This implies $\sigma \propto \tau$ as is given by (3.12). Physically in this stage the increase in gap width is due essentially to the upward flux from the porous bed. For physical insight, we also plot in figure 3 the time history of the ratio of the dimensionless horizontal flux (denoted by Q and

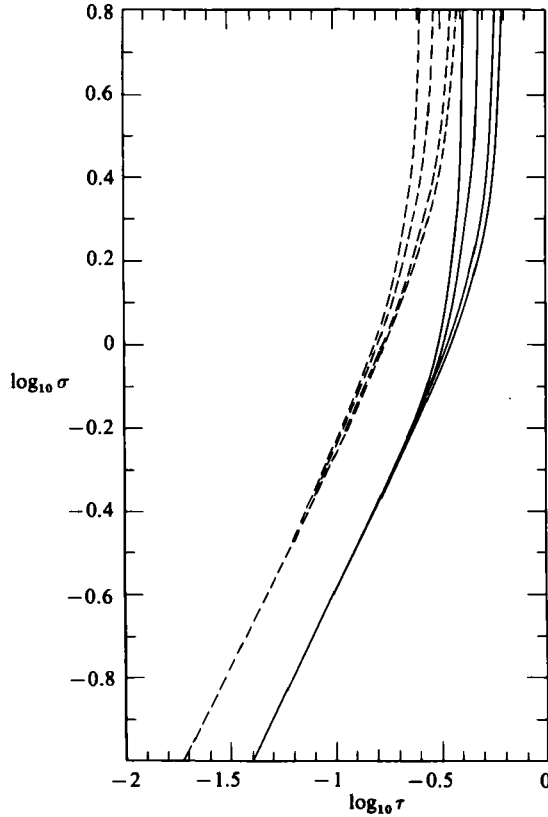


FIGURE 2. $\log_{10} \sigma$ vs. $\log_{10} \tau$ where σ and τ are the dimensionless gap width and time, respectively, as defined in (3.1). Dashed curves are for a wedged gap, and solid curves are for a uniform gap. For each gap, separate curves from left to right correspond to $\beta = 0.1, 1, 10, 100$.

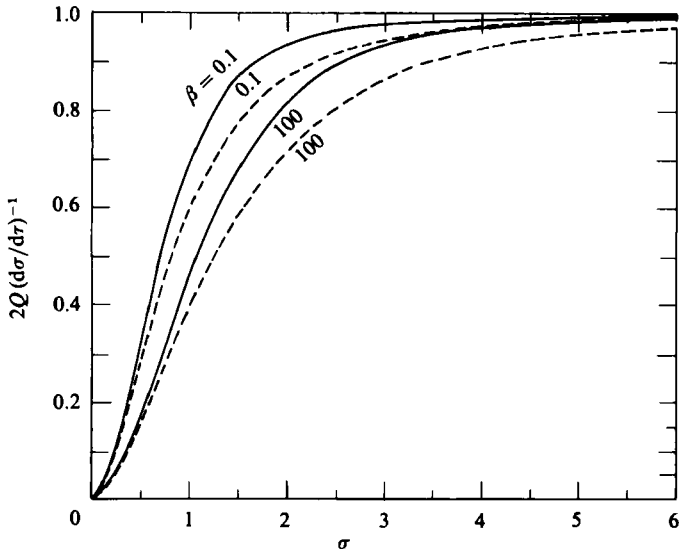


FIGURE 3. Dimensionless horizontal flux Q vs. σ . Q is the second term on the right of (3.14). Dashed curves are for a wedged gap, and solid curves are for a uniform gap.

corresponding to the second term on the right of (3.14)) to the total rate of area increase. It is evident that the breakout time roughly coincides with the time required for the horizontal flux to be the dominant (say 98 %) part of the fluid flux into the gap. From figure 2 an estimate for the breakout time can be obtained: $\tau = \tau_b$, or,

$$T_b = \tau_b(\mu L^{\frac{1}{2}}/Fk^{\frac{1}{2}}) \quad (4.1)$$

where τ_b is a constant depending weakly on the parameter β . For $\beta = 0.1-\infty$, $\tau_b \simeq 0.40-0.62$ for a uniform gap, and $\tau_b \simeq 0.25-0.38$ for a wedged gap. Thus the breakout time is inversely proportional to the applied force in excess of the buoyant weight. For a deformable soil with shear modulus $G = 10^7$ N/m², Foda obtained numerically $t_b \propto F^{1.43}$ for values of $k = 0.3 \times 10^{-8}$ and 0.3×10^{-9} cm², and $L = 10^3$ cm. For these inputs, the breakout time according to (4.1) with $\tau_b = 0.615$ is of the same order of magnitude as Foda's. For example, for $F = 10^5$ (Newtons), $T_b = 100$ s according to Foda (1982, figure 3, for fully saturated pore water); and $T_b \simeq 64$ s from (4.1).

5. Experiments

In order to check the validity of our theory, we have carried out experiments in the laboratory. The experimental setup is sketched in figure 4. A plastic box of 50 cm height, 67 cm length, and 47 cm width was filled with a mixture of water and medium coarse construction sand ($D_{50} = 0.245$ mm) to a thickness of 32 cm. To minimize air entrainment, the mixture was stirred vigorously while being poured into the tank. All the measurements reported here were taken after the soil mass had two months to consolidate. A flat plate of plexiglass of length 45.40 cm and width 15.24 cm was hung on fine steel wires from two identical pulleys of radius 5.00 cm mounted on an axis transverse to the tank. At the midpoint of the axis was a pulley of radius 10.00 cm to which a basket of counterweight was attached. Before the plate was lowered to the top of the soil, the counterweight was exactly equal to the buoyant weight of the plate. A small circular cylinder of height 3.81 cm was fixed on, and protruded up vertically from, the plate to remain in contact with a Hewlett-Packard displacement transducer (Cat. No. DC-DT 7DCDT 7001) whose movement with time was traced on a Gould 2-channel chart recorder. Before each test, water was siphoned out from the top of the soil. The sand surface was smoothed and made horizontal using a scraping device. A thin sheet of water was added barely to cover the sand surface in order to avoid air bubbles beneath the plexiglass plate when being lowered and pressed down. To ensure that the plate was horizontal, the taut steel wires must vibrate with nearly equal amplitude when plucked at the same height by the same force. The sand surface near the plate was smoothed again, especially at the edges. Earlier tests indicated that, when the edges were square, imperfect contact or slight submergence could affect the consistency of results. We therefore machined the lower side of each edge to a sharp angle of 60° to the horizontal; the total contact width was slightly increased to $L = 15.72$ cm. Water was reintroduced slowly until part of the transducer needle was submerged. A given weight was put in the basket while the plate was held down. The chart recorder was started for 10–15 s to attain constant speed, then the plate was released. During the initial stage the chart trace of displacement *vs.* time is a nearly horizontal straight line. When breakout is approached, the chart trace rises sharply. The breakout time is defined by the intersecting point of the final tangent to the trace and the time axis. In view of the long time elapsed, other definitions would lead to only minor differences. Some movement of sand is visible at the moment of breakout.

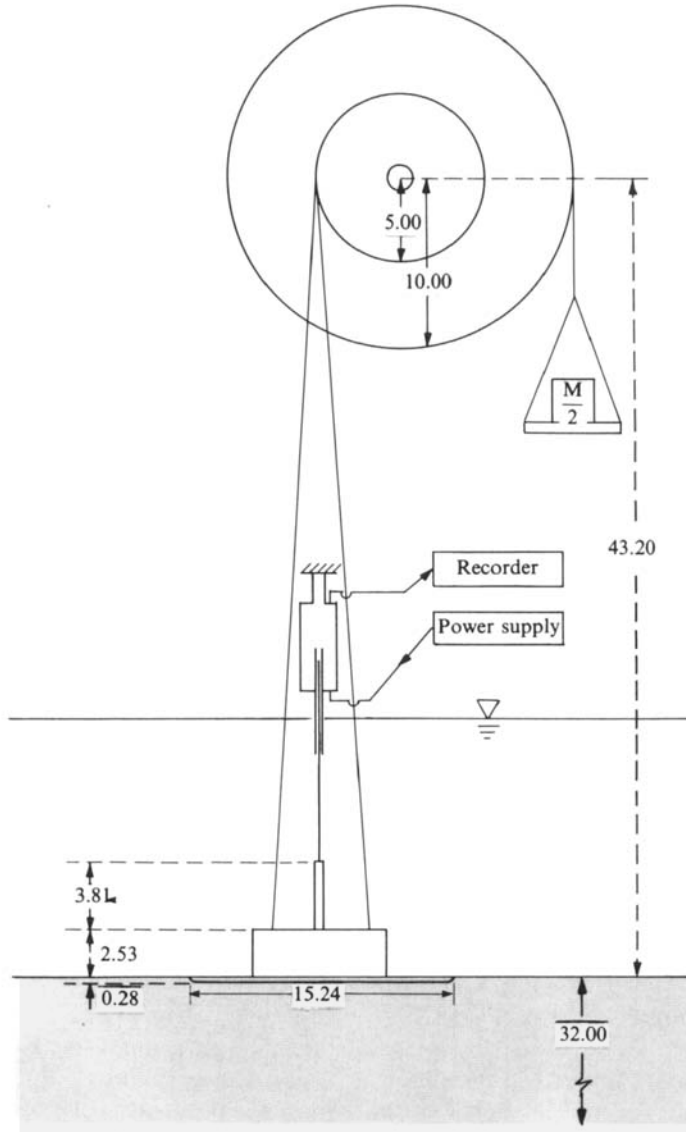


FIGURE 4. Experimental setup. Distances are in cm.

The hydraulic conductivity $K = k(\rho g/\mu)$ of a sand sample from the tank was obtained by a constant head permeometer commonly used in soil mechanics. The temperature of water was also taken. The average result of 3 tests at the same temperature, 19.7°C , is $K = \frac{1}{3}(0.060 + 0.063 + 0.064) \approx 0.062$ cm/s. This permeometer is designed primarily for clay and has a porous screen at the bottom. If the flow has been started for a long time, fine particles can clog the screen and decrease the measured K drastically. Therefore the K values were taken shortly after a steady flow is reached. From this we use the viscosity μ at 19.7°C to compute $k = (\mu/\rho g) K = 0.65 \times 10^{-6}$ cm². Since soil samples taken out of the tank were unavoidably disturbed, we checked our results by the semi-empirical approach of

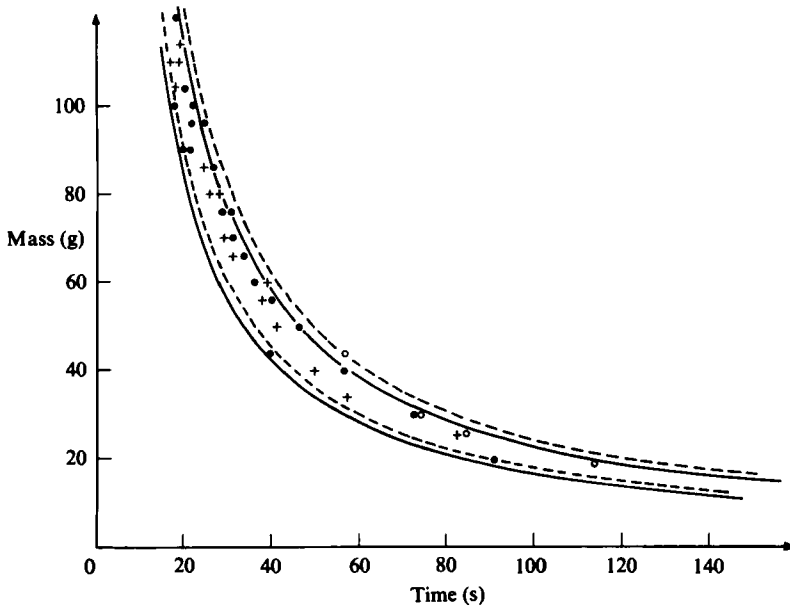


FIGURE 5. Comparison between theory and experiment for the measured break-out time. Mass in g (grams) is twice the mass of the counterweight because of the different pulley radii. Theory: dashed lines, (4.1) using the measured K and at temperature 17 °C; solid lines, (4.1) using the measured K and temperature 20 °C. Experiments: O, temperature range 17–18 °C; ●, 18.1–19 °C; +, 19.1–20 °C. $\beta = \infty$ for upper two curves; $\beta = 0.40$ for lower two curves.

Loudon (1952). Based on extensive experiments with sand in an apparatus initially vacuumed to reduce entrained air, Loudon has found that Kozeny’s formula,

$$K = k \left(\frac{\rho g}{\mu} \right) = \frac{\rho g}{5\mu S^2} \frac{n^3}{(1-n)^2},$$

is reliable. It relates the permeability to the specific surface S of grains (surface area per unit volume of grains) and porosity of soil n . We measured the porosity by taking a volume V of saturated sand and measured its mass before and after being dried in an oven at 50–100 °C for over 16 h. The mass difference gave the porosity:

$$n = (\text{wet mass} - \text{dry mass}) / \rho V,$$

where ρ = density of water. The average of 5 runs was 0.45. In accordance with Loudon, the specific surface was calculated from the formula:

$$S = \sum f_i p_i S_i,$$

where:

- p_i = percentage by weight passing through sieve size i ;
- S_i = surface area of spheres uniformly distributed in size between the mesh d_i and d_{i+1} where d_i is the opening of the last sieve passed and $d_{i+1} < d_i$;
- f_i = shape factor.

Note that for perfect spheres $f_i = 1$. For rounded sand Loudon estimates that $f_i \approx 1.10$, and for angular sand, $f_i \approx 1.40$. Our measured permeability fits Kozeny’s formula if $f_i = 1.17$.

The measured breakout time in seconds is plotted against mass M of the counter weight† in the basket in figure 5. (The force per cm length is $F = Mg/45.40$). The experiments were conducted during a long period in the winter where the water temperature ranged from 17° to 20°, which affects μ in (4.1). Taking the value $k = 0.65 \times 10^{-6} \text{ cm}^2$ we estimate by extrapolating the data of Beavers & Joseph that $\alpha = 0.017$. With the plate width $L = 15.72 \text{ cm}$ we get $\beta = 0.40$; the corresponding τ_b is 0.45. In figure 5 theoretical curves for $\tau_b = 0.45$ and 0.615 are plotted. For each τ_b the dashed curves correspond to 17 °C while the solid curves to 20 °C. Many measured points are seen to be close to the curves for $\beta = \infty$ and lie above the curves for $\beta = 0.40$; this must be due to the fact that during much of the time fluid flow is essentially vertical from below the mud line. The accuracy of the displacement record is about 0.05 cm since the thickness of the pen trace is about 0.03 cm. With reference to figure 2, the dimensional $H(t)$ is related to σ by $H = 0.022\sigma \text{ cm}$, since $k = 0.65 \times 10^{-6} \text{ cm}^2$ and $L = 15.72 \text{ cm}$. If we take $\log_{10} \sigma = 0$ to be the end of the initial stage, the corresponding H is only 0.022 cm, which is too small to compare with experiments meaningfully. In all tests, the values of H at breakout are in the range of 0.15–0.5 cm. The corresponding values of $\log_{10} \sigma$ are in the range 0.80–1.35, which lie on the nearly vertical stretch of the curve in figure 2. Reliable comparison of H vs. t between theory and experiment is therefore very difficult. Because of the long total time from the start, the errors in defining the breakout time in both experiment and theory are small and quantitative comparison is possible.

6. Concluding remarks

Our theory shows that sudden breakout can occur over a porous but rigid seabed. Judging from the field experiments reported by Liu (1969), the total force applied to an object around $L = 2 \text{ m}$ is often just slightly greater than the buoyant weight of the object. The typical net uplift per unit contact area is approximately $O(10^4 \text{ N/m}^2)$ which is far less than the shear modulus of a typical firm sand (10^7 – 10^8 N/m^2). (In our experiments the unit uplift is only 3–15 N/m^2). For still larger objects, the total net uplift force is likely to be an even smaller fraction of the total buoyant weight. Therefore, there must be many practical situations involving large objects, fine firm sands, and small uplift forces, where the small soil displacement (compared to the gap width) allows the assumption of a rigid bed. Of course for smaller objects, it is easier to apply large unit uplift, and soil deformation can be important. In that case however the poro-elastic theory can be quantitatively in error if crude assumptions on the gap geometry are made, as implied by the different results in the two cases treated in this paper. In nature, further complicating factors affecting the adhesion mechanism studied herein can include fluidization and imperfect contact between the body surface and the soil; a more realistic model of the soil/water mixture is needed for a truly satisfactory theory.

Our research has been partially supported by the U.S. National Science Foundation (Grant CME 192-7993) and by the U.S. Office of Naval Research (N-00014-80-C-0531 and -84-K-0026). Part of the work by C. C. Mei was carried out while he was a NTNF Senior Visiting Scientist at the University of Trondheim; the hospitality of the Department of Marine Hydrodynamics, Norwegian Institute of Technology, is acknowledged with pleasure. We are indebted to Prof. Yao Song Chen of Peking

† Because the centre pulley is twice as large as the side pulleys, Mg is twice the actual counter weight added.

University for designing the experimental apparatus. Thanks are also due to Prof. D. R. F. Harleman, whose unpublished records provided much guidance to our own experimental effort, and Dr Jack Germaine for the loan of certain measuring devices.

REFERENCES

- BACHELOR, G. K. 1967 *Introduction to Fluid Dynamics*, Cambridge University Press.
- BEAVERS, G. S. & JOSEPH, D. D. 1976 Boundary condition at a naturally permeable wall. *J. Fluid Mech.* **30**, 197–207.
- FODA, M. A. 1982 On the extrication of large objects from the ocean bottom (the breakout phenomenon). *J. Fluid Mech.* **117**, 211–231.
- LIU, C. L. 1969 Ocean sediment holding strength against breakout of imbedded objects. *Tech. Rep. R-635*, U.S. Naval Civil Engineering Laboratory, Port Hueneme, California.
- LOUDON, A. G. 1952 The computation of permeability from simple soil tests. *Geotechnique* **3**, 165–183.
- MEI, C. C. & FODA, M. A. 1981 Wave induced responses in a fluid filled poro-elastic solid with a free surface – a boundary layer theory. *Geophys. J. R. Astr. Soc.* **66**, 597–631.
- MORSE, P. M. & FESHBACH, H. 1953 *Methods of Theoretical Physics*, vol. 1. McGraw-Hill.
- MUGA, B. J. 1968 Ocean bottom breakout forces, including field test data and the development of an analytical method. *Tech. Rep. R-591*. U.S. Naval Civil Engineering Laboratory, Port Hueneme, California.
- SAFFMAN, P. G. 1971 On the boundary condition at the surface of a porous medium, *Stud. Appl. Maths.* **50**, 93–101.
- TRICOMI, F. G. 1957 *Integral Equations*. Interscience.

